Journal of Photochemistry & Photobiology, A: Chemistry 446 (2024) 115125

Contents lists available at ScienceDirect

Journal of Photochemistry & Photobiology, A: Chemistry

journal homepage: www.elsevier.com/locate/jphotochem

Impact of plasma polymerized Iodine-Doped thiophene films for enhanced sensing response towards industrial VOCs

Baliram Nadekar [a], Yogesh B. Khollam [b], Shoyebmohamad F. Shaikh [c], Ajinkya Trimukhe [d], Rajendra Deshmukh [d], Bidhan Pandit [e,*], Pravin S. More [a,*]

[a] Nanomaterials Application Laboratory, Department of Physics, The Institute of Science, Madam Cama Road, Fort, Mumbai 400032, Maharashtra, India
[b] Department of Physics, Baburaoji Gholap College, Sangvi, Pune 411027, Maharashtra, India
[c] Department of Chemistry, College of Science, Bld-5, King Saud University, Riyadh 11451, Saudi Arabia
[d] Department of Physics, Institute of Chemical Technology, Matunga, Mumbai 400019, Maharashtra, India
[e] Department of Materials Science and Engineering and Chemical Engineering, Universidad Carlos III de Madrid, Avenida de la Universidad 30, 28911 Leganés, Madrid, Spain

ARTICLE INFO

Keywords:
Polythiophene
Iodine doped PPTh
Plasma polymerization system
Volatile organic compounds
Polymeric gas sensing

ABSTRACT

Volatile organic compounds (VOCs) are majorly used in the manufacturing industry and are hazardous to the sustainability of the environment. Polymeric sensors, rather than more traditional metal oxide sensors, are currently taking the lead attention in the greater part of VOC sensing investigations. In polymeric sensors, plasma polymerized thiophene (PPTh) films are being investigated because of their unique properties, wasteless fabrication, and feasibility for commercial mass manufacturing. In the present study, we fabricated PPTh films powered by a 13.6 MHz RF generator with a vacuum level of 10^{-3} Torr in a home-built plasma system. The gas sensor investigation of PPTh and iodine-doped PPTh samples with various VOCs, such as ethanol, methanol, acetone, benzene, toluene, and dichloromethane, was carried out systematically. The iodine-doped PPTh 10–20 films (48 hr) showed the highest sensitivity for ethanol (~180) and methanol (~120) as compared to PPTh for ethanol (~110) at 1000 ppm gas concentration. A sensitivity degradation study over 60 days revealed the long-term stability of the films in the air. The polar hopping mechanism and decreased charge transport centers after reaction with the hydroxyl group are responsible for resulted sensitivity of iodine-doped PPTh films towards alcohols.

1. Introduction

Plasma is considered the fourth state of matter. It contains ionized gas, but overall, it is electrically neutral. The polymerization of monomer material using the plasma state of the monomer is called plasma polymerization. In plasma polymerization, thermal or electrical energy is applied to monomer vapours, which creates a mixture containing electrons, ions, radicals, and neutral species of the monomer material [1]. For plasma polymerization, cold plasma is preferred over hot plasma with a 1 % degree of ionization as cold plasma can be sustained at room temperature without any expensive apparatus. It also prevents the thermal degradation of polymer material [2]. In a vacuum chamber, the monomer material is converted into reactive fragments, which recombine to form a polymer and can be deposited on a substrate of any shape [3]. Plasma polymerization is a dry polymerization method and does not involve any solvent. This makes plasma polymerized materials free of any chemical impurity. Plasma polymerization does not create any by-products or waste materials, making it the most environmentally friendly polymerization technique. The thickness of layers deposited depends directly on the deposition time and monomer flow rate for a particular polymerization system, making it easily controllable [4]. The properties of plasma polymerized materials can be altered using chamber temperature, monomer flow, source RF power, duty cycle, and pressure [5]. Due to the high degree of cross-linking, plasma polymers can be insoluble, thermally stable, and strong [6].

The VOCs are majorly used in the manufacturing industry as raw materials. The VOCs released into the environment by these industries contribute greatly to pollution and are hazardous to the sustainability of life for humans and other species. Earlier sensing studies focused on toxic gases like carbon monoxide, nitrogen dioxide, hydrogen, and

* Corresponding authors.
E-mail addresses: bpandit@ing.uc3m.es (B. Pandit), pravin.more@iscm.ac.in (P.S. More).

https://doi.org/10.1016/j.jphotochem.2023.115125
Received 28 April 2023; Received in revised form 21 August 2023; Accepted 28 August 2023
Available online 3 September 2023

ammonia [6]. Still, their focus has been extended to detecting VOCs in recent years due to their significant use in industrial and domestic sectors. Classically used metal oxide-based sensors suffer many problems when it comes to the effective sensing of VOCs. Low sensitivity and poor selectivity are the major issues as the number of VOCs is present simultaneously in the environment [7]. The metal oxide-based sensors have to be maintained at higher temperatures to function properly, which consumes much power. Nowadays, many polymer compounds are being developed to study and apply their variety of physical and electrical properties. The reversible or irreversible changes in physical or chemical properties of polymers in the presence of external stimuli are interesting in many application fields [8 –9]. M.F. Mabrook et al. reported a sensitivity of 88 for ethanol and 68 for methanol using inkjet-printed polypyrrole at 5000 ppm [10]. Jaber Nasrollah Gavgani et al.; established a methanol sensitivity of 120 and ethanol sensitivity of 40 using Poly(3,4-ethylenedioxythiophene) composites at 50 ppm [11]. Chemically polymerized materials have been effectively employed for VOC sensing [12]. X. Guo and team fabricated the polythiophene/WO_3 sensor to study the sensitivity towards the NO_2. In their study they recorded the sensitivity of 60 for 0.16% concentration of NO_2. They reported highest sensitivity at room temperature compared to elevated temperatures [13]. S. Bai and team synthesised polythiophene and WO_3 hybrid to detect the H_2S at room temperature. They recorded the response of 14 for 100 ppm of H_2S. The response is multiplied by 10 after forming polythiophene-WO_3 composite compared to only polythiophene films. This highlights the sensing abilities of polythiophene composites as a sensing element [14]. Because of this, the objective of the present work is to optimize the cost-effective and wasteless plasma polymerization of thiophene monomer and study its characteristics in sensing environmentally hazardous VOCs, which are handled in large quantities by manufacturing industries. Polythiophene is the attractive polymer material that has shown promising results in ammonia, nitrogen dioxide, hydrogen sulfide sensing. When iodine is doped into polymer material, it changes the amount of charge carrier centres in the polymer film. Formation of vapours in resublimed iodine makes it easier to dope it into already fabricated plasma polymerized thin films. Herein, we prepared PPTh and iodine-doped PPTh via a home-built plasma polymerization technique (Fig. 1). The structure and surface morphology of the as-prepared PPTh and iodine-doped PPTh were studied using various methods before being used in gas sensor applications (Fig. 2). In comparison to PPTh film, the content of iodine-doped PPTh films improves gas sensor performance. A mechanism for the improved gas performance in iodine-doped PPTh has been presented as well including proper discussions of materials and methods discussed in supporting information.

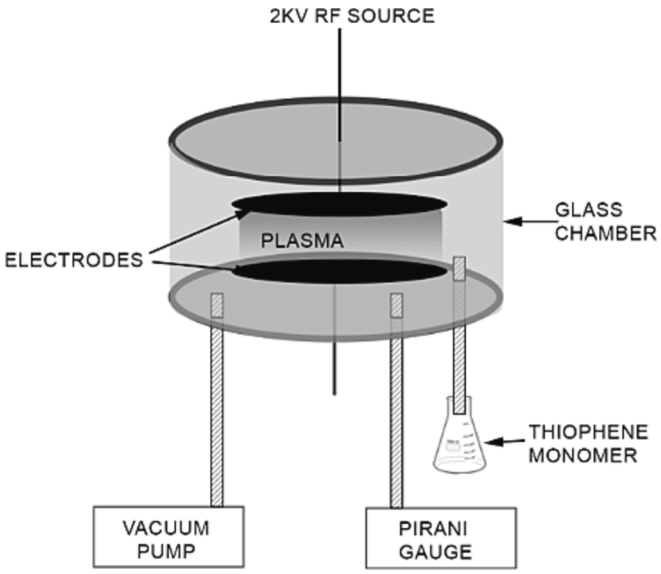

Fig. 1. Schematic diagram for home-built plasma polymerization system.

2. Materials and methods

2.1. Fabrication of iodine doped PPTh film sensor

The glass substrate was used to fabricate the PPTh samples due to their high thermal and chemical stability. AR grade thiophene monomer and resublimed iodine was obtained from SD Fine Chemical Ltd, India. Thorough cleaning process was used to remove any chemical, physical and organic contamination from the glass substrates. Method of plasma polymerization was used to fabricate the PPTh samples. Fig. 1 shows the home-built plasma polymerization system powered by 2 kV RF power source and 13.6 MHz frequency. Pulsed plasma was used to deposit the samples of PPTh. The pulse frequency and duty cycle were varied to deposit the different films of plasma polymerized thiophene. The four films deposited at different duty cycles were identified as (1) PPTh 5–10 (5 ms ON − 10 ms OFF), (2) PPTh 10–20 (10 ms ON − 20 ms OFF), (3) PPTh 10–50 (10 ms ON − 50 ms OFF), and (4) PPTh 10–100 (10 ms ON − 100 ms OFF) and subjected for further studies. After preliminary studies PPTh 10–20 film was doped with iodine for 2 hr, 8 hr 16 hr and 48 hr. For iodine doping, samples were placed in a closed chamber with resublimed iodine crystals and iodine vapours were used to dope the samples.

2.2. Characterization of iodine doped PPTh film sensor

Material characterization of PPTh and iodine doped PPTh films was carried out using XRD (XPERT-PROMPD, CuKα radiation, λ = 1.5405 Å), FTIR (Perkin Elmer Spectrum Two with UATR), SEM (JEOL JSM-IT300LV) and laser microscope (Olympus DSX 1000). Gas sensor characterization was done using home-built four probe-based gas sensing system. The gas sensing system uses Keithley 2400 sourcemeter to measure the resistivity of the sensor films. The sensitivity of the sensor can be defined as the percentage ratio of the change in resistance in presence of analyte gas to the original resistance of the sensor. Selectivity of the gas sensor is its ability to differentiate between two different analyte gases. The high selectivity of the sensor finds its origin in difference in activation energies of material in presence of different gases. The activation energy here indicates the amount of energy required to transport the charge carriers in presence of specific gaseous environment. Higher activation energy values indicate need of more energy to transport charge carriers through the sensor film and vice versa [15–16].

$$Sensitivity = \left|\frac{R_a - R_g}{R_a}\right| \times 100$$

$$\text{Selectivity} = \frac{S_{g1}}{S_{g2}}$$

$$\text{Activation energy} = \log\frac{R_g T}{1000}$$

R_a and R_g are the resistances of the film in the presence of air and gas 'g', respectively. S_{g1} and S_{g2} are sensitivities for gas 1 and gas 2 and 'T' is the operating temperature.

3. Results and discussion

3.1. X-ray diffraction and FTIR analysis

Fig. 3 (a) shows the X-ray diffraction (XRD) patterns of all pure PPTh films at different pulsed plasma. All the XRD patterns show a broad peak between 15°-35°, which indicates the amorphous nature of plasma-polymerized thiophene PPTh films. All pure PPTh films with different

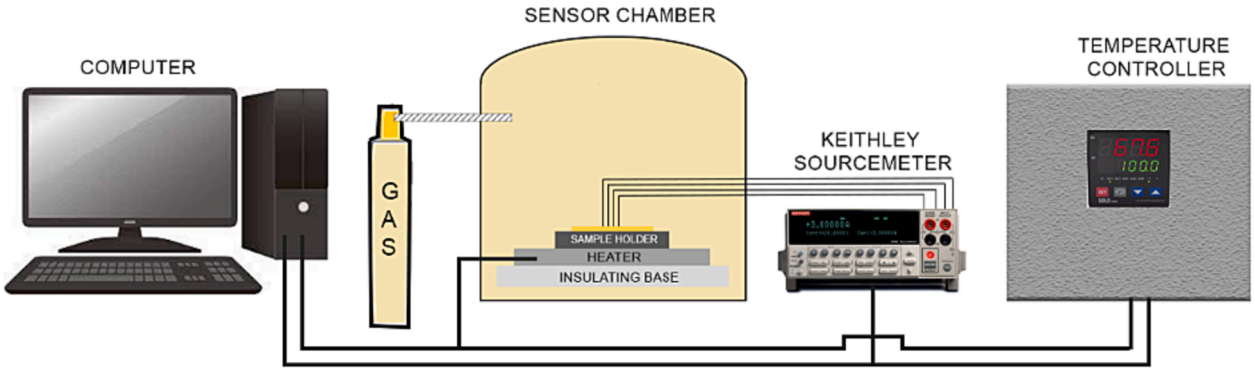

Fig. 2. Schematic diagram for home-built four-probe based static gas characterization system.

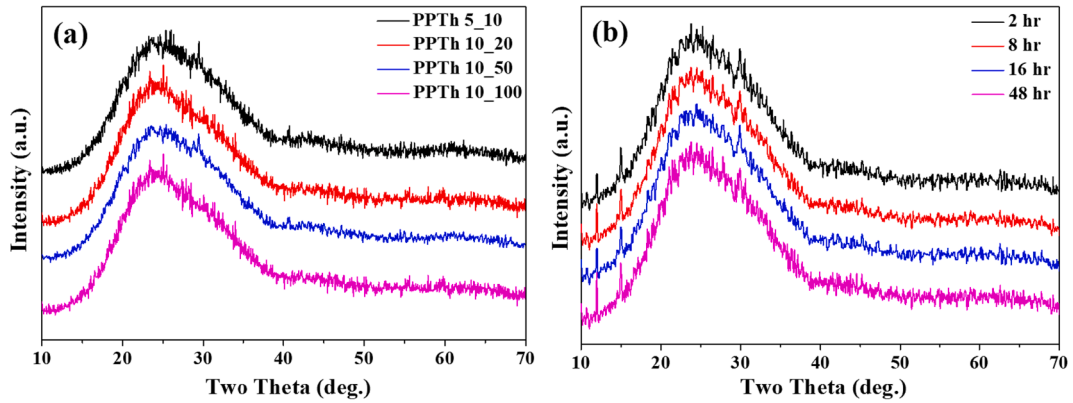

Fig. 3. X-ray diffraction patterns for (a) PPTh 5–10, PPTh 10–20, PPTh 10–50 & PPTh 10–100 films and (b) PPTh 10–20 films doped with iodine for 2 hr, 8 hr, 16 hr & 48 hr.

pulsed plasma show similar XRD patterns, indicating no notable structural difference in plasma polymerized films even after varying the duty cycle of deposition. Fig. 3 (b) shows the XRD patterns of PPTh 10–20 films doped with iodine for different doping times of 2 hr, 8 hr, 16 hr, and 48 hr. The XRD patterns for PPTh 10–20 films doped with iodine show reflection at $2\theta = 11.9°$ and 14.9°. These are the reflection due to presence of the iodine present on the PPTh film. The sharp peaks indicate the non-amorphous nature of the iodine in iodine doped PPTh films.

Fig. 4(a) shows the FTIR spectra for undoped PPTh films. In all FTIR spectra, two peaks observed at 1447 cm^{-1} and 1041 cm^{-1} represent the stretching vibrations in the thiophene ring. It shows that some part of the ring structure of thiophene is preserved. This indicates that all undoped PPTh films are in the form of polythiophene. The peak at 3410 cm^{-1} typically belongs to the hydroxyl group indicating thereby the presence of water molecules in the resultant films possibly absorbed from the environment. The peaks at 1262 cm^{-1} and 1040 cm^{-1} primarily represent sulphur-oxygen and carbon–oxygen bonds present in polythiophene. The C = C bonding with the alkyl group is identified with peaks at 618 cm^{-1} to 900 cm^{-1}. The methyl and methylene groups are represented by peaks at 2928 cm^{-1} and 2963 cm^{-1}. The thiol ester, amide, carboxyl, and carbonyl are represented by peaks at 1622 cm^{-1} and 1661 cm^{-1} [3]. All the peaks present in FTIR spectra of undoped films are also present in FTIR spectra of PPTh 10–20 films doped with iodine for different times of 2 hr, 8 hr, 16 hr, and 24 hr, as shown in Fig. 4 (b). With increasing doping time, the intensities of different peaks are observed to be increasing. The plasma polymerization radicals are

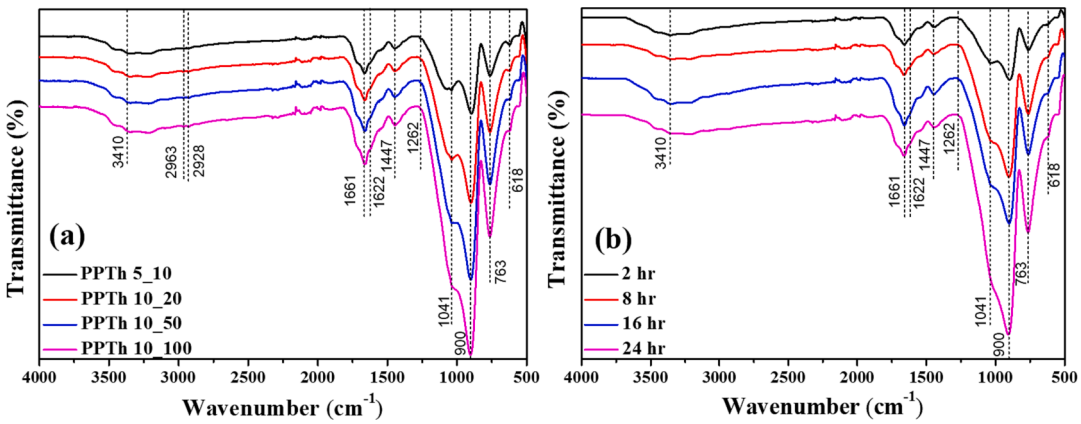

Fig. 4. FTIR patterns for (a) PPTh 5–10, PPTh 10–20, PPTh 10–50 & PPTh 10–100 films and (b) PPTh 10–20 films doped with iodine for 2 hr, 8 hr, 16 hr & 48 hr.

formed by fragmentation of monomer, which could be responsible for the absence of some functional groups from the FTIR spectra.

3.2. SEM analysis

Fig. 5 (a), (b), and (c) show the scanning electron microscope (SEM) images at x1500 magnification for PPTh 10–20 film doped with iodine for 2 hr, 8 hr, 16 hr, respectively. Fig. 5 (d), (e), and (f) show SEM images for PPTh 10–20 film doped with iodine for 48 hr at different magnifications of x1500, x12000, and x20000 respectively. From Fig. 5 (a) to (d), it is clear that all SEM images show polymer complex branches or granular structures connected on the surface of PPTh 10–20 films doped with iodine. The density of these polymer complex branches or granular structures increases with increasing iodine doping time from 2 hr to 48 hr as is seen in Fig. 5 (a) to (d). The SEM images are given in Fig. 5 (d) to (f) for PPTh 10–20 films doped with iodine under different magnifications indicating granular structures in particles with spherical morphology. The average size of the spherical granules is 200 nm as seen in Fig. 5(f).

Classically, in metal oxide-based gas sensors, a non-uniform surface is preferred as it increases the surface area, and hence more gas is absorbed in sensing to increase sensitivity. With polymer materials, sensitivity is already measurable, non-uniform surfaces or increasing surface area with porous surfaces is not absolutely necessary [17–19]. In plasma polymerization, two major aspects controlling the film's resistivity are the film's thickness and the uniformity of the surface. As seen in morphological studies, PPTh 10–20 films doped with iodine already have a uniform surface. The thickness of the film can be effectively controlled by monitoring the deposition time and flow rate of monomer material. Hence, in the present case, the spherical granular structures obtained might be useful for enhancing the sensitivity of the films after doping.

3.3. Laser microscopy analysis

Fig. 6 (a), (b) (c), and (d) give the laser microscopy images at 20000X magnification for the PPTh 10–20 film doped with iodine for 2 hr, 8 hr, 16 hr, and 48 hr, respectively. The 3D laser microscopy images reveal that the surfaces of the iodine-doped PPTh 10–20 films are highly uniform. The blue-coloured parts of all images stand for the uniform base material deposition. The yellow-orange coloured spots seen in Fig. 6 (a)-(d) scattered across the surfaces of different films show small non-uniformities in the film surface. Even though these yellow-orange coloured spots are present all over the surface, the collective surface area of these spots is negligible compared to the total surface area of the given film. The maximum height of these spots is calculated from the uniformly deposited surface of the film, and it is found to be 4 μm. As the doping time increases, the surface topography also changes, and the effect of doping on topography can be seen in the images. Fig. 6 (e) shows the graph for height profile data over the scanned length for the PPTh 10–20 films doped with iodine for 48 hr [20]. The average thickness of the PPTh 10–20 film doped with iodine for 48 h is 20.73 μm.

3.4. Gas sensing analysis

3.4.1. Sensitivity of pure PPTh films for different VOCs

Fig. 7 shows the sensitivity of PPTh 5–10, PPTh 10–20, PPTh 10–50, and PPTh 10–100 films for different VOCs: ethanol, methanol, acetone, benzene, toluene, and dichloromethane at 1000 ppm of each. From this Fig. 7, it is clear that only PPTh 10–20 has the highest values of sensitivities for ethanol, methanol, acetone, benzene, toluene, and dichloromethane compared to the corresponding values for other films of PPTh 5–10, PPTh 10–50, and PPTh 10–100. The sensitivities for ethanol, methanol, acetone, benzene, toluene, and dichloromethane are 110, 71, 14, 24, 17, and 26. The sensitivities for the ethanol and methanol are higher than acetone, benzene, toluene, and dichloromethane for PPTh 10–20 film. Hence for further studies, PPTh 10–20 film is selected. The PPTh 10–20 film is doped with iodine at different doping times of 2 hr, 8 hr, 16 hr, and 48 hr and subjected to VOC sensing characteristics studies.

3.4.2. Sensitivity of iodine-doped PPTh films for different VOCs

Fig. 8 shows the sensitivity variation with doping time for PPTh 10–20 films doped with iodine for 2 hr, 8 hr, 16 hr, and 48 hr. The

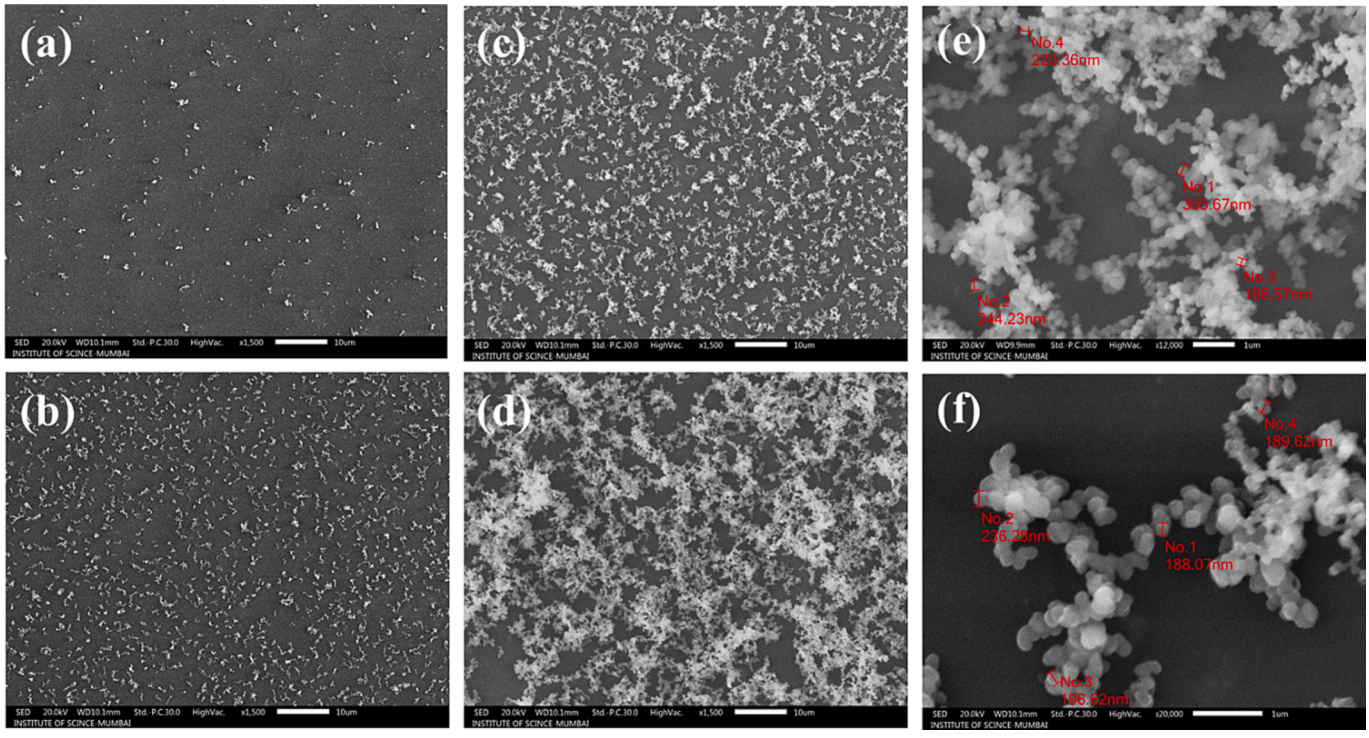

Fig. 5. SEM images for PPTh 10–20 films doped with iodine for (a) 2 hr, (b) 8 hr, (c) 16 hr, and (d)-(f) 48 hr at different magnifications.

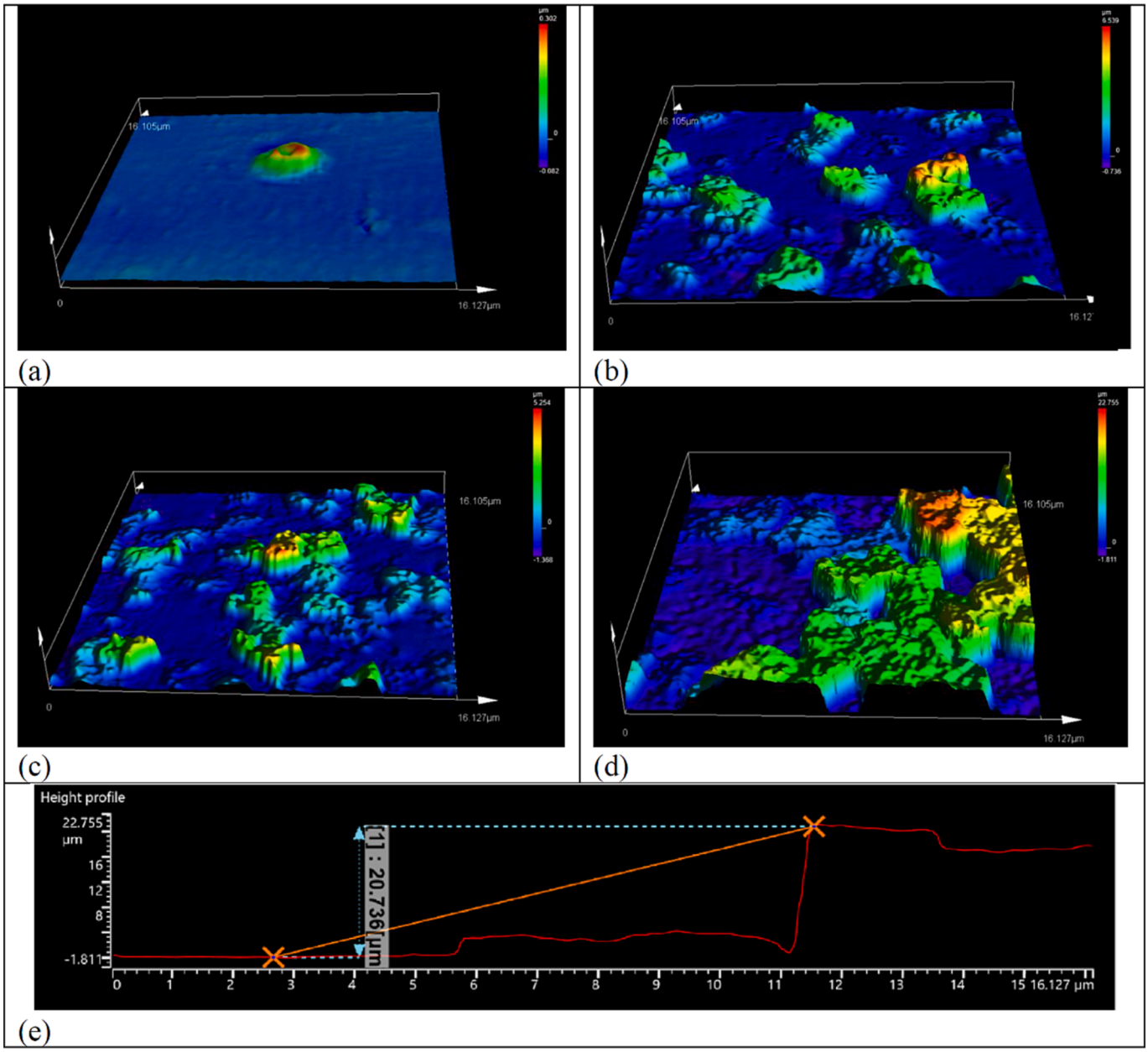

Fig. 6. (a), (b), (c), and (d) laser microscopy images for PPTh 10–20 films doped with iodine for 2 hr, 8 hr, 16 hr & 48 hr at 20000X magnification respectively, and (e) height profile of PPTh 10–20 films doped with iodine for 48 hr.

sensitivities increase with increasing doping time for all VOCs. In the case of acetone, benzene, toluene, and dichloromethane, the increase in sensitivities concerning the doping time is very small compared to ethanol and methanol. For ethanol and methanol, the sensitivities increase continuously and significantly with doping time. For PPTh 10–20 films doped with iodine for 2 hr, the sensitivities are ~ 25 for ethanol and ~ 20 for methanol (Fig. 8). The highest values of sensitivities equal to 183 for ethanol and 124 for methanol are found for the PPTh 10–20 films doped with iodine for 48 h. This can be termed saturation doping, as the iodine atoms acquire almost all the available sites for doping. This study shows sensitivity reaches a maximum after the saturation doping of iodine, and the highest sensitivity is recorded for ethanol and methanol. For the PPTh 10–20 films doped with iodine for 48 hr, the sensitivities values for acetone, benzene, toluene, and dichloromethane are observed to be 12, 21, 16, and 4 respectively. The sensitivities towards ethanol and methanol change almost two times after the iodine doping of PPTh 10–20 films. This establishes ethanol and methanol sensing dominance for further experimental evaluation of PPTh 10–20 films doped with iodine.

3.4.2.1. Selectivity of iodine-doped PPTh films for ethanol and methanol w. r.t. Different VOCs. The selectivity of polymer-based sensors is an important aspect, which makes them a dominant choice over metal oxide-based gas sensors. Fig. 9 shows the histogram for the selectivity of ethanol and methanol over other VOCs of acetone, benzene, toluene, and dichloromethane. Both; ethanol and methanol show better selectivity over the other VOCs of acetone, benzene, toluene, and dichloromethane.

3.4.2.2. The activation energy for iodine-doped PPTh films for different VOCs. Fig. 10 gives the activation energy data for PPTh 10–20 films doped with iodine for 48 hr in different VOCs. The activation energy values for ethanol and methanol are 8.088 kJ/mol and 8.054 kJ/mol, respectively, which are higher than that for the air and other VOCs of

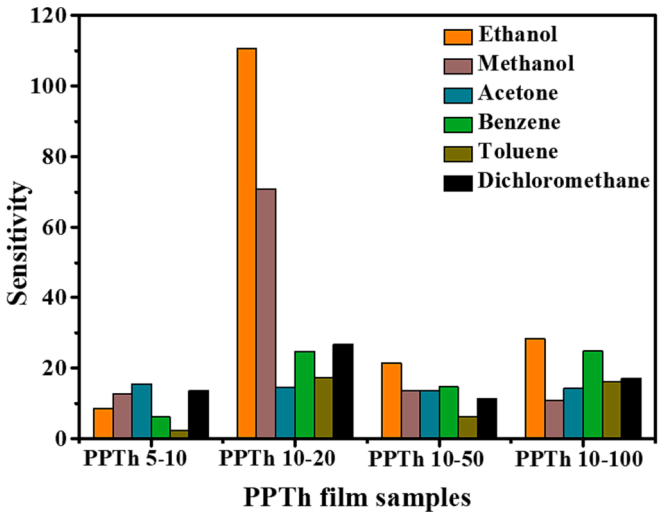

Fig. 7. Sensitivity for PPTh 5–10, PPTh 10–20, PPTh 10–50, and PPTh 10–100 films for different VOCs: ethanol, methanol, acetone, benzene, dichloromethane, and toluene (at 1000 ppm of each).

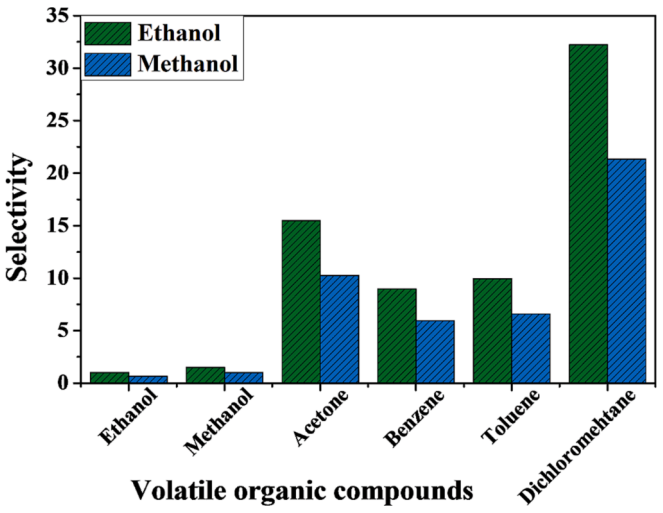

Fig. 9. Selectivity for PPTh 10–20 films doped with iodine for 48 h for ethanol and methanol for different VOCs: acetone, benzene, dichloromethane, and toluene.

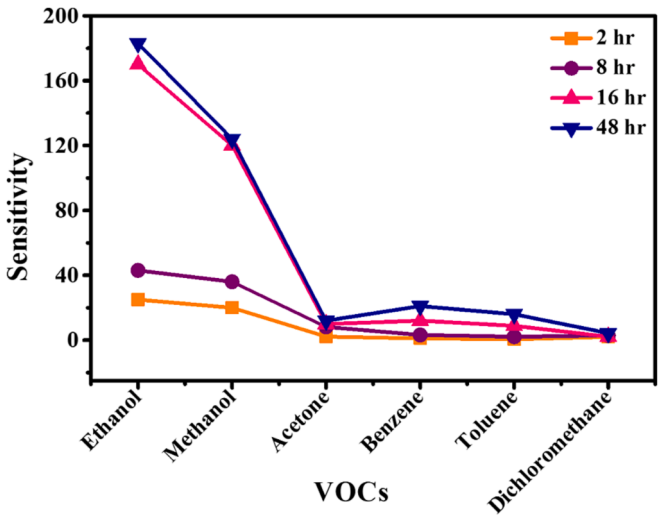

Fig. 8. Variation of sensitivity for PPTh 10–20 films doped with iodine for 2 hr, 8 hr, 16 hr, and 48 hr for different VOCs: ethanol, methanol, acetone, benzene, dichloromethane, and toluene (at 1000 ppm of each).

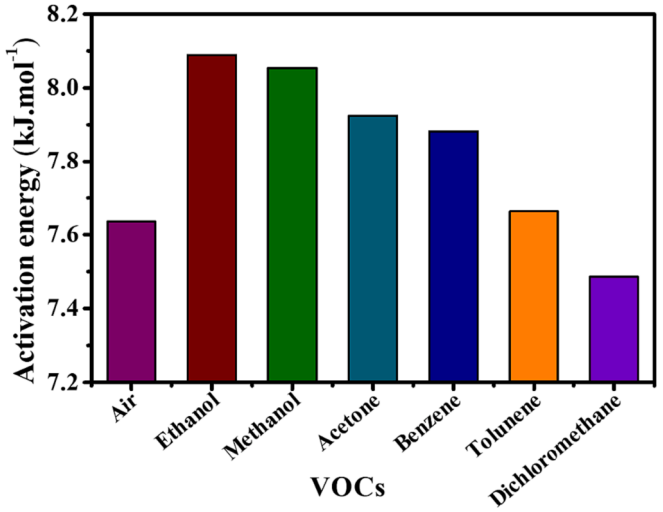

Fig. 10. Activation energy for iodine-doped PPTh film for 48 hr for different VOCs: ethanol, methanol, acetone, benzene, dichloromethane, toluene, and air.

acetone, benzene, toluene, and dichloromethane. It implies that more energy is needed to transport the charge carriers in presence of ethanol and methanol gases, contributing to increased resistivity compared to air and other VOCs of acetone, benzene, toluene, and dichloromethane [21]. Difference in the activation energy in presence of different analyte gases is the reason for the origin of detected selectivity for alcohols over other gases like acetone, benzene, toluene and dichloromethane.

3.4.2.3. Sensing repeatability of iodine-doped PPTh 10–20 film for ethanol and methanol VOCs. The repeatability measurements are carried out only for the iodine-doped PPTh 10–20 film and those VOCs showing the highest sensing characteristics. For repeatability measurements, the four cycles of sensitivity versus time are recorded throughout 1200 s. Fig. 11 shows the sensitivity versus time repeatability curves for iodine-doped PPTh 10–20 film for 48 hr for ethanol and methanol VOCs (at 1000 ppm of each). The sensing cycles are repeatable with a certain degree of random error, and repeatability for ethanol sensing is noted to be better than that for methanol. The reversibility of iodine-doped PPTh 10–20 films for ethanol and methanol sensing can be observed in Fig. 11. Although initial resistance is almost reached again after exposing the films to the air atmosphere in the last 300 s of each cycle, there is a change in base resistance of films after each cycle, which persists until the end of the cycle. The average response time and recovery time are 300 s and 150 s, respectively, for each sensing cycle.

3.4.2.4. Temperature, time, and concentration-dependent sensitivity of iodine-doped PPTh 10–20 film for ethanol and methanol VOCs. Temperature plays an important role in gas sensors, as classically used sensors must be maintained at high temperatures [22]. The polymer materials such as PPTh used in the present study can operate at ambient temperature for sensing applications. However, to establish the needlessness for temperature control, it is necessary to study the stability of these sensors at different temperatures. Fig. 12 (a) provides sensitivity versus operating temperature variation for PPTh 10–20 films doped with iodine for 48 hr for ethanol and methanol VOCs (at 1000 ppm of each). Fig. 12 (a) shows no major fluctuations in the sensitivities of ethanol and methanol even if the operating film temperature is changed from 35 °C to 70 °C. It indicates that the PPTh 10_20 films doped with iodine are highly stable even elevated temperature. There is no need to monitor or

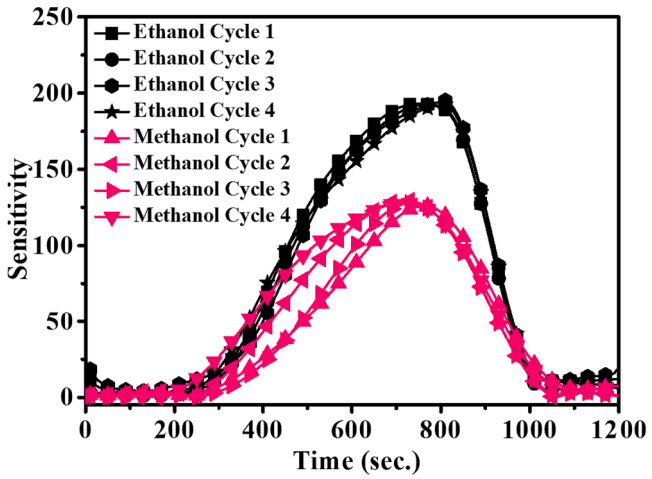

Fig. 11. Repeatability: variation of sensitivity vs. time at four cycles for PPTh 10–20 films doped with iodine for 48 hr for ethanol and methanol VOCs (at 1000 ppm of each).

maintain a particular temperature for their effective operations. The best operating temperature for the iodine-doped PPTh film gas sensor would be an ambient temperature of around ~ 30 °C. This setup would not need any special mechanism to maintain a specific temperature for effective operations of iodine doped PPTh gas sensor.

Another important disadvantage of classically used sensor materials is their instability for long-period operations, as sensors tend to start losing their sensing ability if operated for a longer time. To study this aspect in the case of PPTh 10–20 films doped with iodine, a sensor degradation study is carried out over 60 days. Fig. 12 (b) gives sensitivity variation versus the number of days for iodine-doped PPTh 10–20 film for 48 hr in ethanol and methanol VOCs (at 1000 ppm of each). Initially, on day-0, the films are studied immediately after the iodine doping, and the sensing response is recorded. The highest values of sensitivities are found to be ~ 300 for ethanol and ~ 150 for methanol. These values are higher than the average sensitivity recorded for ethanol and methanol in our experiment, possibly because of excess iodine present on the film. On day-5, the sensitivity values are reduced to ~ 200 for ethanol and 118 for methanol. These are stable sensitivities for ethanol and methanol. On day-10, sensitivity is not affected considerably. These sensitivity values stay almost stable for 30 days. From day-5 to day-60, sensitivities for both ethanol and methanol are reduced by only 15 % to 17 %. It indicates that ethanol and methanol sensing performances of iodine-doped PPTh 10–20 film for 48 hr are stable over the period of 60 days. When the sensor film is exposed to air for a long duration, other environmental gases may interact with the sensor film. This contaminates the sensor film and reduces the adsorption of analyte gas molecules. This results in a reduction in sensitivity after operating the sensor for longer durations.

Fig. 12 (c) shows the variation of sensitivity versus concentration of ethanol and methanol VOCs (in ppm) for iodine-doped PPTh 10–20 film for 48 hr at 50 ppm concertation sample shows the sensitivity of 9 for methanol and 8 for ethanol. At 100 ppm concentration, the sensitivity values for ethanol and methanol are ~ 11 to ~ 13, respectively. The sensitivities for methanol and ethanol are almost similar, up to 500 ppm. A huge change is recorded in sensitivities at 1000 ppm, with methanol sensitivity at 127 and ethanol sensitivity at 193. Until this point sensitivity is found directly proportional to the concentration in the ppm range. At 2000 ppm sensing ability of samples is found to be somewhat saturated. Methanol sensitivity only increases to 165, and ethanol sensitivity reaches 230 at 2000 ppm.

3.4.2.5. Vocs sensing process and mechanism. The XRD results indicated the amorphous nature of the PPTh 10–20 and iodine-doped PPTh 10–20 film. This amorphous structure is effective in gas sensing as the gas sorption reaction generates charge carriers on the film surface. Fig. 13 (a) depicts the process of VOC sensing by PPTh and iodine-doped PPTh 10–20 films. The accumulation of charge carriers at grain boundaries of

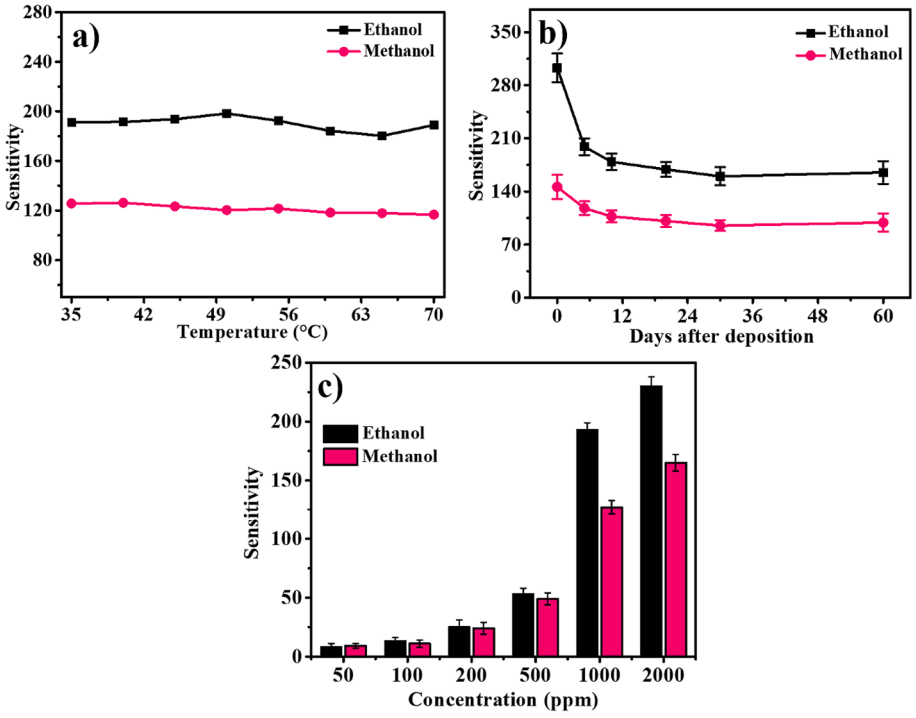

Fig. 12. (a) Variation of sensitivity vs. operating temperature for iodine-doped PPTh 10–20 film for 48 hr for ethanol and methanol VOCs (at 1000 ppm of each), (b) Variation of sensitivity vs. the number of days for iodine-doped PPTh 10–20 film for 48 hr for ethanol and methanol VOCs (at 1000 ppm of each), and (c) Variation of sensitivity vs. concentration (in ppm) of VOCs: ethanol and methanol for iodine doped PPTh 10–20 film for 48 hr.

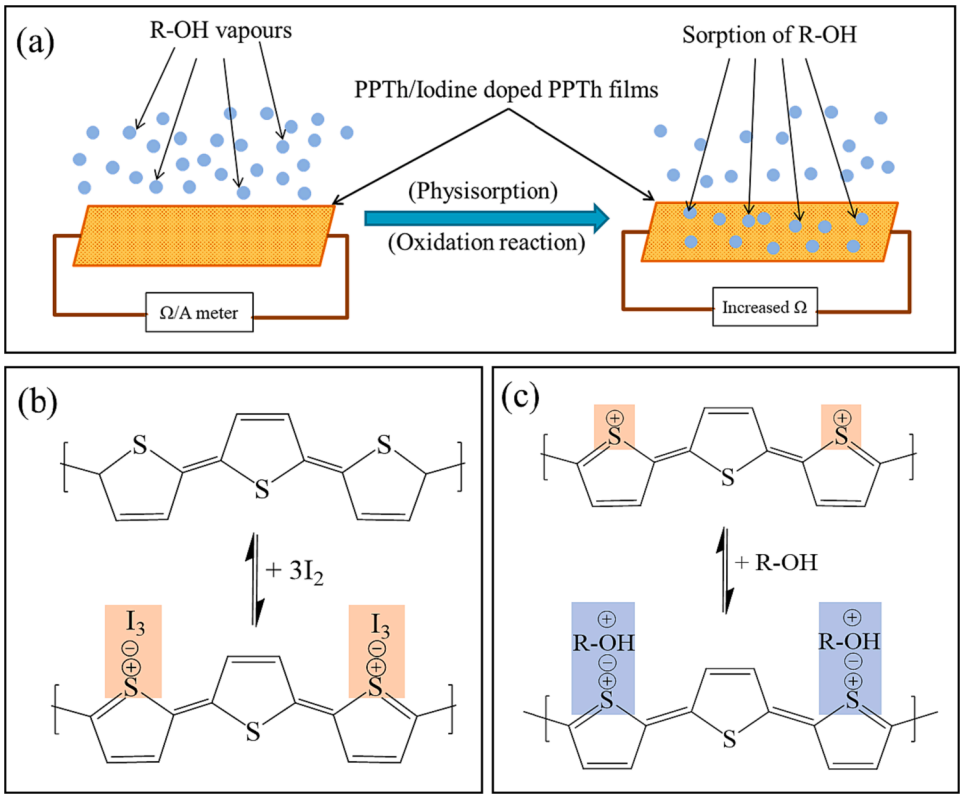

Fig. 13. (a) Alcohol sensing process (b) Mechanisms for iodine doping of PPTh films, (b) Alcohol sensing mechanism for the sensor using iodine doped PPTh films.

such amorphous material amplifies the change in resistivity during gas sensing. Such grain boundaries of amorphous materials have conductivity several orders higher than the non-amorphous materials [23].

In conjugated polymers like polythiophene, the polar hopping process is the mechanism for conductance in intra-chain and inter-chain charge transportation [24]. The doping of plasma polymerized thiophene (PPTh) film with iodine creates positive charge centres. Fig. 13 (b)-(c) gives the mechanisms for iodine doping of PPTh films, and VOCs sensing by iodine-doped PPTh films. The conduction in PPTh film is enhanced due to iodine doping as it removes an electron from the aromatic rings of PPTh [6]. The major charge carrier density is also increased in the process. The ethanol and methanol contain a hydroxyl group, an electron donor. During the sensing of ethanol or methanol VOCs, the hydroxyl group reacts with the PPTh or iodine-doped PPTh films, which may decrease the charge transport centres on the film surface and grain boundaries. This results in increased film resistivity. This effect is more in the case of iodine-doped PPTh film due to higher charge carrier density than the pure PPTh film. The depletion of charge carriers causes localized bending in the valance and conduction band. After PPTh 10–20 films doped with iodine are exposed to ethanol or methanol, their molecules are physisorbed by the film, and the potential of hopping polarons is changed. The changes in resistance of the film are also associated with the rearrangement of the PPTh structure and deprotonation of thiophene sites [5].

4. Conclusions

The plasma polymerized Thiophene films was fabricated with varied pulse frequency and duty cycles at room temperature. Iodine doping was employed to enhance the conductivity and overall sensitivity of PPTh films toward studied VOCs. FTIR confirms the formation of plasma-polymerized thiophene as bonds specific to thiophene rings are detected. SEM and optical microscopy categorized iodine-doped PPTh 10–20 film surfaces as highly uniform. PPTh 10–20 films doped with iodine show high sensitivity towards ethanol and methanol while comparatively inactive for other VOCs under study. Temperature stability enables these films to be operated at any given temperature in the range 30℃ to 70℃ without monitoring the surrounding temperature. PPTh 10–20 films doped with iodine were stable for a longer period without any major changes in sensitivity.

CRediT authorship contribution statement

Baliram Nadekar: Investigation, Writing & editing. **Yogesh B. Khollam:** Resources, Project administration, Software. **Shoyebmohamad F. Shaikh:** Review and editing, Resources, Formal analysis. **Ajinkya Trimukhe:** Resources, Formal analysis. **Rajendra Deshmukh:** Resources, Formal analysis. **Bidhan Pandit:** Validiation, Resources. Playing role of suprevisions. **Pravin S. More:** Investigation, Writing – review & editing, Playing role of suprevisions.

Declaration of Competing Interest

The authors declare that they have no known competing financial interests or personal relationships that could have appeared to influence the work reported in this paper.

Data availability

Data will be made available on request.

Acknowledgments

This research is funded by the Rajiv Gandhi Science and Technology Commission, Mumbai, Maharashtra, India (File No: RGSTC/File2016/DPP-146/CR-36). The authors are thankful to the University Grant Commission (UGC) New Delhi, India, for financial support in terms of the major research project and also thankful to the Department of

Science and Technology (DST) for supporting the Department of Physics, The Institute of Science under the scheme of Fund for Improvement of S & T Infrastructure (FIST). The authors would like to thank the researchers supporting project number (RSP2023R370), King Saud University, Riyadh, Saudi Arabia, for financial support. The authors also sincerely thank KIST School Partnership Project, Seoul, South Korea. Bidhan Pandit acknowledges the CONEX-Plus programme funded by Universidad Carlos III de Madrid (UC3M) and the European Commission through the Marie-Sklodowska Curie COFUND Action (Grant Agreement No 801538). Bidhan Pandit also acknowledges Universidad Carlos III de Madrid (Read & Publish Agreement CRUE-CSIC 2023) for funding the article processing charge (APC) to make this article open access.

References

[1] J. Friedrich, Mechanisms of Plasma Polymerization - Reviewed from a Chemical Point of View, Plasma Process. Polym. 8 (2011) 783–802, https://doi.org/10.1002/ppap.201100038.
[2] C. Alemán, G. Fabregat, E. Armelin, J.J. Buendía, J. Llorca, Plasma surface modification of polymers for sensor applications, J. Mater. Chem. B. 6 (2018) 6515–6533, https://doi.org/10.1039/C8TB01553H.
[3] M. Silverstein, I. Visoly-Fisher, Plasma polymerized thiophene: molecular structure and electrical properties, Polymer (Guildf). 43 (2002) 11–20, https://doi.org/10.1016/S0032-3861(01)00582-1.
[4] L.M.H. Groenewoud, G.H.M. Engbers, J.G.A. Terlingen, H. Wormeester, J. Feijen, Pulsed Plasma Polymerization of Thiophene, Langmuir. 16 (2000) 6278–6286, https://doi.org/10.1021/la000111b.
[5] C.M. Hussain, Handbook of Nanomaterials for Industrial Applications, Elsevier (2018), https://doi.org/10.1016/C2016-0-04427-3.
[6] H. Bai, G. Shi, Gas Sensors Based on Conducting Polymers, Sensors. 7 (2007) 267–307, https://doi.org/10.3390/s7030267.
[7] Y. Yan, G. Yang, J.-L. Xu, M. Zhang, C.-C. Kuo, S.-D. Wang, Conducting polymer-inorganic nanocomposite-based gas sensors: a review, Sci. Technol. Adv. Mater. 21 (2020) 768–786, https://doi.org/10.1080/14686996.2020.1820845.
[8] S. Cichosz, A. Masek, M. Zaborski, Polymer-based sensors: A review, Polym. Test. 67 (2018) 342–348, https://doi.org/10.1016/J.POLYMERTESTING.2018.03.024.
[9] U. Lange, N.V. Roznyatovskaya, V.M. Mirsky, Conducting polymers in chemical sensors and arrays, Anal. Chim. Acta. 614 (2008) 1–26, https://doi.org/10.1016/j.aca.2008.02.068.
[10] M.F. Mabrook, C. Pearson, M.C. Petty, Inkjet-printed polypyrrole thin films for vapour sensing, Sensors Actuators B Chem. 115 (2006) 547–551, https://doi.org/10.1016/j.snb.2005.10.019.
[11] J.N. Gavgani, H.S. Dehsari, A. Hasani, M. Mahyari, E.K. Shalamzari, A. Salehi, F. A. Taromi, A room temperature volatile organic compound sensor with enhanced performance, fast response and recovery based on N-doped graphene quantum dots and poly(3,4-ethylenedioxythiophene)–poly(styrenesulfonate) nanocomposite, RSC Adv. 5 (2015) 57559–57567, https://doi.org/10.1039/C5RA08158K.
[12] M. Tomić, M. Šetka, L. Vojkůvka, S. Vallejos, VOCs Sensing by Metal Oxides, Conductive Polymers, and Carbon-Based Materials, Nanomaterials. 11 (2021) 552, https://doi.org/10.3390/nano11020552.
[13] X. Guo, K. Yan-fei, Y. Tai-li, W. Shu-rong, Low-temperature NO2 sensors based on polythiophene/WO3 organic-inorganic hybrids, Transactions of Nonferrous Metals Society of China 22 (2) (2012) 380–385, https://doi.org/10.1016/S1003-6326(11)61187-4.
[14] S. Bai, K. Zhang, J. Sun, D. Zhang, R. Luo, D. Li, C. Liu, Polythiophene-WO3 hybrid architectures for low-temperature H2S detection, Sensors and Actuators B: Chemical 197 (2014) 142–148, https://doi.org/10.1016/j.snb.2014.02.038.
[15] B.S. Nadekar, G.S. Gund, Y.B. Khollam, S.F. Shaikh, D.S. Wavhal, D.P. Dubal, P. More, Plasma-Polymerized and Iodine-Doped Polyvinyl Acetate for Volatile Organic Compound Gas Sensing Applications, ACS Appl Polym Mater. 5 (2023) 1882–1890, https://doi.org/10.1021/acsapm.2c01963.
[16] Z. A. Piskulich, O. O. Mesele, W. H. Thompson, Removing the barrier to the calculation of activation energies: Diffusion coefficients and reorientation times in liquid water, J. Chem. Phys. 147, (2017) 134103. https://doi.org/10.1063/1.4997723.
[17] X. Liu, S. Cheng, H. Liu, S. Hu, D. Zhang, H. Ning, A Survey on Gas Sensing Technology, Sensors. 12 (2012) 9635–9665, https://doi.org/10.3390/s120709635.
[18] C.S. Park, D.H. Kim, B.J. Shin, D.Y. Kim, H.K. Lee, H.S. Tae, Conductive Polymer Synthesis with Single-Crystallinity via a Novel Plasma Polymerization Technique for Gas Sensor Applications, Mater. 2016, Vol. 9, Page 812. 9 (2016) 812. https://doi.org/10.3390/MA9100812.
[19] H. Li, J. Dailey, T. Kale, K. Besar, K. Koehler, H.E. Katz, Sensitive and Selective NO 2 Sensing Based on Alkyl- and Alkylthio-Thiophene Polymer Conductance and Conductance Ratio Changes from Differential Chemical Doping, ACS Appl. Mater. Interfaces. 9 (2017) 20501–20507, https://doi.org/10.1021/acsami.7b02721.
[20] H.J. Jang, C.-S. Park, E.Y. Jung, G.T. Bae, B.J. Shin, H.-S. Tae, Synthesis and Properties of Thiophene and Aniline Copolymer Using Atmospheric Pressure Plasma Jets Copolymerization Technique, Polymers (Basel). 12 (2020) 2225, https://doi.org/10.3390/polym12102225.
[21] M.G. Olayo, G.J. Cruz, S. López, J. Morales, R. Olayo, Conductivity and Activation Energy in Polymers Synthesized by Plasmas of Thiophene, J. Mex. Chem. Soc. 54 (2019) 18–23. https://doi.org/10.29356/jmcs.v54i1.960.
[22] S.A.S., . P.S.M., . D.J.L., . R.W.R., Investigation of PEG embedded WO3-graphene thin film sensor, Adv. Mater. Proc. 2 (2021) 506–509. https://doi.org/10.5185/amp.2017/807.
[23] K. Claus-Dieter, W. Thorsten, Gas sensing fundamentals. Springer 15 (2014) 1–46, https://doi.org/10.1007/5446-2013-56.
[24] B. Li, S. Santhanam, L. Schultz, M. Jeffries-EL, M.C. Iovu, G. Sauvé, J. Cooper, R. Zhang, J.C. Revelli, A.G. Kusne, J.L. Snyder, T. Kowalewski, L.E. Weiss, R. D. McCullough, G.K. Fedder, D.N. Lambeth, Inkjet printed chemical sensor array based on polythiophene conductive polymers, Sensors Actuators B Chem. 123 (2007) 651–660, https://doi.org/10.1016/j.snb.2006.09.064.

Bidhan Pandit is now a Marie Curie CONEX-Plus researcher at University Carlos III de Madrid (UC3M), Madrid, Spain. He received his Ph.D. degree (2019) in Physics from Visvesvaraya National Institute of Technology (India) and joined as CNRS Postdoctoral Research Fellow at the Institut Charles Gerhardt Montpellier (ICGM), Université de Montpellier (France). His previous scientific interests focus on the synthesis of nanostructures and fabrication of flexible devices for supercapacitor applications. His current research focus includes the synthesis of cathode materials for lithium, sodium and potassium-ion batteries, as well as the *in situ/operando* X-ray based characterizations for the understanding of battery mechanisms.